Vol. 718: 119–136, 2023
https://doi.org/10.3354/meps14374

MARINE ECOLOGY PROGRESS SERIES
Mar Ecol Prog Ser

Published September 7

Habitat use of the northern bottlenose whale *Hyperoodon ampullatus* near Jan Mayen, North Atlantic

K. Y. Woo[1,2], S. Isojunno[1,3], P. J. O. Miller[1,*]

[1]Sea Mammal Research Unit, Scottish Oceans Institute, University of St. Andrews, St. Andrews, Fife KY16 8LB, UK

[2]*Present address:* APEM Ltd, The Technopole Centre, Edinburgh Technopole, Milton Bridge, Nr Penicuik, Midlothian EH26 0PJ, UK

[3]*Present address:* Centre for Research into Ecological and Environmental Modelling (CREEM), University of St Andrews, The Observatory, Buchanan Gardens, St. Andrews, KY16 9LZ, UK

ABSTRACT: Habitat use of the northern bottlenose whale *Hyperoodon ampullatus* in the Northeast Atlantic is poorly understood. This study aimed to identify locally utilised habitat features and create predictions of northern bottlenose whale habitat use over a wider area around the island of Jan Mayen, Norway. Bottlenose whales were sighted regularly near Jan Mayen in June 2014–2016 at higher rates than over a wider study region reported in other studies, indicating that the Jan Mayen habitat may be a hotspot of bottlenose whale presence in early boreal summer. Habitat models were created by fitting generalised additive models of selected environmental variables to sighting occurrence and additional whale sightings given a first encounter (total number of sightings − 1) recorded in June 2014–2016. Higher occurrence was estimated at steeper topography and April-average chlorophyll concentration below 0.4 mg m^{-3}. Additional whale sightings given a first encounter were predicted to be higher at water depths (<1000 m) with steep topography, and deeper water (depths between 1300 and 2000 m) with a gentle seafloor slope. Spatial predictions largely corresponded with field observations that indicated high usage around the submarine canyon regions in the east and southeast of Jan Mayen Island. This study highlights the likely importance of steep and deep bathymetric features in shaping patterns of habitat use of this deep-diving species. Predictions of habitat use over a wider area not covered by the analysed surveys require validation; however, these data could inform conservation and management efforts to minimise spatial overlap between potential high-use areas and potentially disruptive anthropogenic activities.

KEY WORDS: Habitat use · Habitat models · Beaked whale · Multi-model inference · Generalised additive models · Bathymetry · Opportunistic sampling · North Atlantic

1. INTRODUCTION

Patterns of habitat use reflect the way animals utilise the geographic and biological distribution of resources (Krausman 1999). For wide-ranging mobile animals such as cetaceans, responses to environmental variability are readily reflected by spatial and temporal changes in distribution and habitat-use patterns (Forney 2000). Species–habitat modelling can serve as a powerful and flexible tool to explain and predict such varying patterns of habitat use under ecologically dynamic processes (Forney 2000, Redfern et al. 2006) and thus allow inference of high-use areas with respect to associated environmental features (Guisan & Zimmermann 2000). Together with knowledge of distribution and abundance (Hooker et al. 1999,

*Corresponding author: pm29@st-andrews.ac.uk

Cañadas et al. 2005, Redfern et al. 2006, Rogan et al. 2017), understanding habitat use sets a foundation for effective conservation and management. For example, habitat-based mitigation measures can reduce spatial and temporal overlap between areas of high animal occurrence and anthropogenic activities (Rogan et al. 2017). However, it can be challenging to obtain the required field data for offshore deep-diving marine mammals such as beaked whales because of the financial and logistical constraints involved with studying these elusive species (Forney 2000).

Cetacean distribution within their feeding areas is expected to be primarily correlated with the abundance and distribution of their prey (Kenny et al. 1996, Hátún et al. 2009), which may be largely unknown (e.g. Isojunno et al. 2012). Therefore, environmental variables are usually included in habitat models as proxy measurements of prey availability (Redfern et al. 2006, Rogan et al. 2017). The northern bottlenose whale *Hyperoodon ampullatus* (Forster, 1770) (Family Ziphiidae, beaked whales), hereafter referred to as the 'northern bottlenose whale', is a deep-diving cetacean for which scarce information on distribution and habitat use is available owing to biological factors such as its pelagic habitat (Hooker et al. 2002, Ramírez-Martínez et al. 2019) and long and deep dives (Hooker & Baird 1999). Previous studies indicate that they feed primarily on the benthic-living cephalopod *Gonatus fabricii*, the most abundant deep-water squid in the Arctic and sub-Arctic (Bjørke 1995), and occasionally on other squid species and fish (Kastelein & Gerrits 1991, Lick & Piatkowski 1998, Hooker et al. 2001, Fernández et al. 2014). Knowledge of population trends and distribution of this species is principally based upon historical whaling records (Whitehead et al. 2021) and recent research on the uniquely well-studied population in the Gully, Nova Scotia, Canada (Hooker 1999, Gowans et al. 2000). Likely driven by prey distribution and availability, bottlenose whales tend to favour open waters of ≥1000 m depth along the continental slope (Benjaminsen 1972, Whitehead & Hooker 2012), the primary habitat of large and mature *G. fabricii* (Bjørke 2001).

More than 65 000 bottlenose whales were killed during commercial whaling beginning in the 1850s (Reeves et al. 1993). This has severely depleted the global population, likely causing them to remain well below historical levels (Whitehead et al. 2021) given their slow reproductive rate (Feyrer et al. 2020). In combination with high susceptibility to pervasive anthropogenic threats, including disturbance from underwater noise (Miller et al. 2015a, Wensveen et al. 2019) and risk of bycatch, bottlenose whales are classified as Near Threatened on the IUCN Red List (Whitehead et al. 2021). Currently, no regional or national conservation framework has been established for this species or its habitat outside the Gully Marine Protected Area (Whitehead & Hooker 2012), where bottlenose whales of the Scotian Shelf are found to be genetically distinct from other North Atlantic populations (COSEWIC 2011, Feyrer 2021, de Greef et al. 2022, Einfeldt et al. 2022).

In the Northeast Atlantic, where bottlenose whales were most hunted (Whitehead & Hooker 2012), estimates from the 1990s indicated roughly 40 000 individuals (NAMMCO 1995), with a high-latitude (over 60° N) population potentially forming 4 distinct stocks off (1) northern eastern Greenland, Iceland, Jan Mayen and Faeroe Islands, (2) Andenes, Norway, (3) Møre, Norway, and (4) Svalbard (Benjaminsen 1972, Whitehead & Hooker 2012). Recent sightings data have documented bottlenose whales in waters southeast of Svalbard and along the Knipovich Ridge (Storrie et al. 2018). High-density areas were identified in shipboard line-transect surveys between the British Isles and Greenland, but few or no sightings were made in historic whaling grounds off Svalbard, Andenes, and Møre, despite survey effort in those areas (Ramírez-Martínez & Hammond 2019). The northern limits for this species in the eastern North Atlantic may be in a state of flux due to changing ice conditions (Whitehead et al. 2021). A broad description of habitat use in the northeast Atlantic based on shipboard surveys conducted in 1998–2015 found a positive effect of depths from 800 to 2000 m on bottlenose whale density, with waters shallower than 500 m having a negative effect on whale density (Ramírez-Martínez & Hammond 2019). Other significant factors included seafloor aspect, sea surface temperature (SST), and mixed layer depth in June, salinity in August, sea surface height (SSH) in July, and chlorophyll *a* (chl *a*) in April.

From 2014 to 2016, the $3S^3$-ORBS (sea mammals and sonar safety — off-range beaked whale study) project (Miller et al. 2014, 2015b, 2016) conducted sailboat-based surveys in the waters off the Island of Jan Mayen to collect visual sightings and animal-attached tag data from bottlenose whales. During the survey period in June of each year, animals were routinely sighted along the Jan Mayen submarine canyon, mainly to the north and southeast of the island of Jan Mayen. The surveyed area is topographically dominated by the West Jan Mayen Fracture Zone, which forms a steep submarine canyon (1200–3800 m; see Fig. 1) (IHO–IOC 2017), resulting in a steep and deep bathymetric profile close to the

north coast of Jan Mayen Island. Oceanographically, the region is characterised by the Nordic Sea circulation, which consists mainly of the warm and saline Norwegian Atlantic current and the cold and fresh East Greenland current flowing in opposite directions (Piechura & Walczowski 1995, De Schepper et al. 2015). The interface between these currents forms the Arctic Jan Mayen front (Piechura & Walczowski 1995, Børsheim et al. 2014, Erga et al. 2014), which creates a strong thermohalocline gradient within the water column from 0 to 200 m (Piechura & Walczowski 1995). The spring bloom off northern Jan Mayen is found to last longer and reach higher chlorophyll concentrations than other regions on the Arctic side of the front (Børsheim et al. 2014).

The aims of this study were to (1) use bottlenose whale sightings data to quantify habitat use near Jan Mayen and identify key static and dynamic environmental correlates of bottlenose whale presence within a habitat-use model, and (2) apply the habitat-use model to predict potential bottlenose whale habitat-use patterns across a wider area of the Greenland Sea.

2. MATERIALS AND METHODS

2.1. Surveyed area and wider prediction area

The surveyed area encompassed a marine region covered by major survey effort tracks around the island of Jan Mayen in the Norwegian Sea (Fig. 1), delimited by latitudes 70–71.5° N and by longitudes 5–9.5° W. Model predictions were made over a wider rectangular marine region demarcated by latitudes 68–72° N and by longitudes 1–17° W, based on sightings made within the surveyed area.

2.2. Visual sighting data collection

Visual sighting data of bottlenose whales were collected in June in 2014, 2015, and 2016 (Table 1), with search effort concentrating along the submarine canyon from north to southeast of Jan Mayen Island (Fig. 1). Visual surveys were conducted by 2 dedicated observers from the deck whenever weather

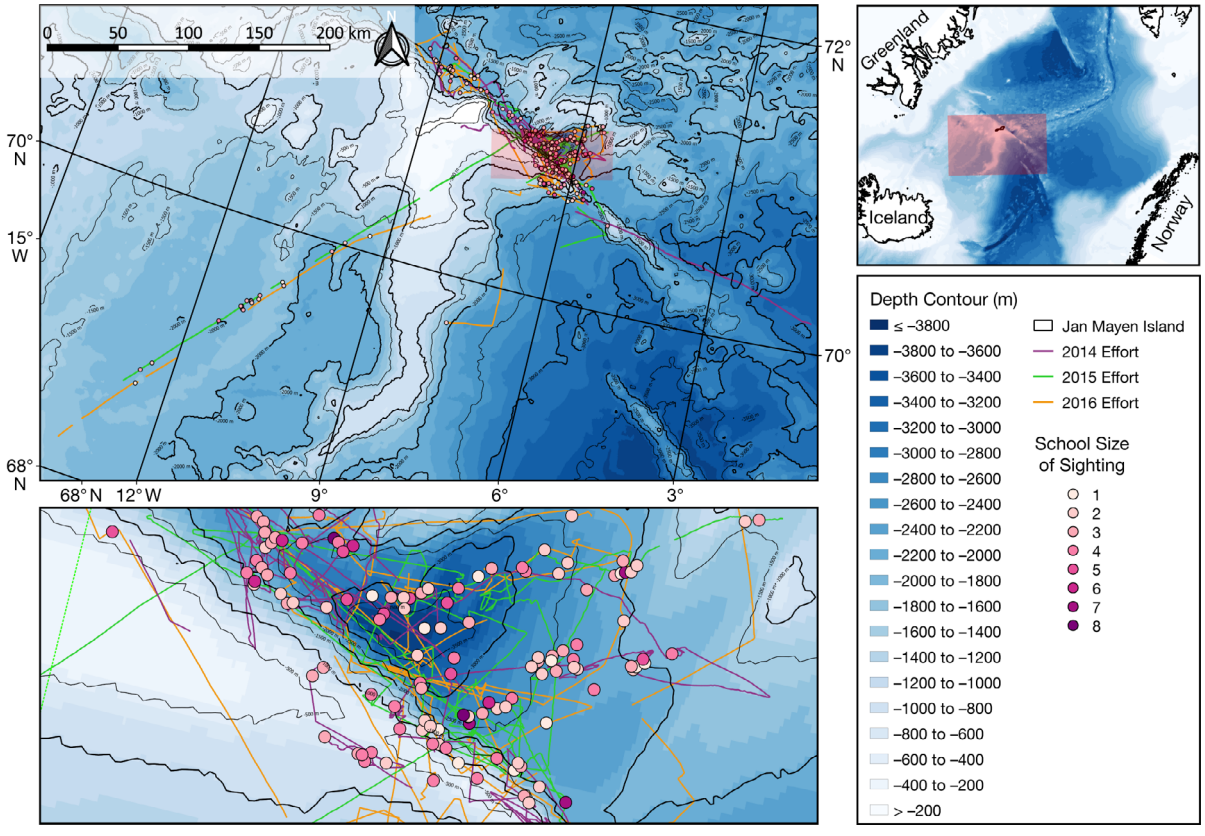

Fig. 1. (Top left) Location and number of northern bottlenose whale sightings (coloured symbols) and survey effort (coloured lines) by year within the study area off Jan Mayen Island. (Top right) location of the study area relative to Iceland, Greenland and Norway. (Bottom left) Zoomed map illustrating the dense sighting records made along the submarine canyon to the southeast of Jan Mayen Island

Table 1. Selected survey effort and northern bottlenose whale sightings by year

	2014	2015	2016	Total
Start date of survey	10 June	15 June	2 June	–
End date of survey	26 June	2 July	24 June	–
Research vessel and length	T/S 'Prolific' (29 m)	'Donna Wood' (32 m)	'Donna Wood'	–
Survey duration (h)	166.0	152.4	201.1	519.5 h
Distance surveyed (km)	1237.4	1137.4	1574.9	3949.7
Number of sightings	77	75	68	220
Average group size of whale sightings	3.01 ± 1.11	3.08 ± 1.59	3.19 ± 1.59	3.09 ± 1.44
Number of 12.5 km effort segments	99	91	126	316
Number of segments with sightings	46	31	37	114

conditions permitted. Both observers made visual scans from bow to stern, with one observer searching across the starboard and the other across the port of the boat, together covering 360° around the vessel. Binoculars were used to confirm whale species and location once an animal was spotted.

When a sighting was made, the time, whale location (latitude and longitude), estimated sighting distance, bearing, group size, animal heading, and level and duration of seeking (behavioural indication of attractive movement towards the research vessel, as suggested by Whitehead & Hooker 2012) were recorded. Vessel GPS location and speed were automatically logged every 5 s in 2014 and 2015, and every 1 s in 2016.

Boat speed was maintained between 4 and 7 knots during the survey, which was approximately double that of the normal swim speed of bottlenose whales (~5 km h^{-1}; Kastelein & Gerrits 1991). Therefore, it could be assumed that animals were stationary when visual sampling took place, and any positive bias due to repeated counting of the same individual or group was minimised (Glennie et al. 2015).

Following a sighting, the whales were often approached for tagging. If successful, the tagged whale would be tracked for the duration of the tag deployment. Sighting and effort data during tagging and tracking periods were excluded from the analyses.

2.3. Calculation of survey effort

Survey effort, which is a measure of locations searched, was first quantified to account for the spatial and temporal heterogeneity of sampling, which was opportunistic in the sense that it was determined mostly by weather and logistics for tagging, rather than *a priori* distribution survey design. Only effort data with Beaufort sea state lower than 5 and visibility greater than 2 km, when observers actively looked for whales during on-effort status, were considered for further analysis. These criteria were used to reduce perception bias caused by poor weather conditions. The selected tracks were then divided into segments of 12.5 km, with each segment representing a spatial unit of observer effort. The 12.5 km segment length was determined considering the size of the study area and the average spatial resolution of explanatory variables so that covariate values were not over-averaged within each effort segment.

2.4. Tabulation of static and dynamic environmental variables

Effort segments were populated with a covariate set of grid pixels on which the centroid point of each segment landed, based on the assumption that whale sighting and its corresponding effort segment shared the same set of environmental variables. A grid layer of 1470 pixels (12.5 × 12.5 km) was overlaid on the wider prediction area to standardise the spatial resolution of environmental variables for each grid cell. As grid size was the same as the length of an effort segment, candidate covariates were not over-averaged within an effort segment and were also not averaged over several effort segments. Environmental predictors that were evaluated for inclusion in habitat-use models consisted of 5 static, 4 dynamic, and 2 temporal covariate variables (Table 2).

2.4.1. Static environmental variables

Bathymetry was summarised as water depth (BODC 2003), seafloor slope, aspect, and distance from 2000 m depth contours. It was expected that underwater topography would play a considerable role in explain-

Table 2. Predictor variables for habitat models of sighting presence and additional northern bottlenose whale sightings given a first encounter

Variable	Spatial resolution	Temporal resolution	Description	Data source
Static predictor variables				
Depth.m	30 arc-sec	N/A	Average water depth (in m)	Gridded bathymetry data from General Bathymetric Chart of the Oceans (GEBCO), obtained from interpolated depth soundings from ship (BODC 2003)
Slope.max	30 arc-sec	N/A	Maximum degree of seafloor inclination from the horizontal surface (angle, in degrees)	Derived from GEBCO gridded bathymetry data
Aspect	30 arc-sec	N/A	Average seafloor orientation in which the slope is facing (in number degrees of east, increasing counter-clockwise)	Derived from GEBCO gridded bathymetry data
DistAF	N/A	N/A	Distance from the Arctic front (in km)	Steady distance values calculated based on the location of Arctic Front illustrated by Piechura & Walczowski (1995), and Børsheim et al. (2014)
Dist2000	N/A	N/A	Distance from the nearest 2000 m contour (in km). Positive value for sample point located at water depth ≥2000 m; negative value for point at water depth <2000 m	Derived from GEBCO gridded bathymetry data
Dynamic predictor variables				
Chl *a*	1 × 1 km	Monthly averaged (April)	Average sea surface chl *a* concentration in 2014–2016 (in mg m^{-3})	Monthly mean satellite data of global ocean chlorophyll (global colour processor) provided by the EU Copernicus Marine Service Information
SST	0.25 × 0.25 degree	As above	Average sea surface temperature in 2014–2016 (in K)	Daily mean *in situ* and satellite ensemble products of global ocean sea surface temperature from 11 analysis systems. Data obtained from the EU Copernicus Marine Service Information
SSH	0.083 × 0.083 degree	As above	Average sea surface height (in m) above geoid in 2014–2016	Daily mean numerical model data of sea surface height assimilated using the Incremental Analysis Update (IAU) method. Data obtained from the EU Copernicus Marine Service Information
SA	0.083 × 0.083 degree	Monthly averaged (June)	Average sea surface salinity in 2014–2016 (10^{-3})	Daily mean numerical model data of salinity assimilated using the Incremental Analysis Update (IAU) method. Advection of the salinity tracers was computed with the total variance diminishing advection scheme. Data obtained from the EU Copernicus Marine Service Information
Temporal predictor variables				
Solar elevation	N/A	Hourly	Solar position in terms of sun elevation angle measured up from the horizon (in degrees)	Calculated based on the algorithm provided by Michalsky (1988)
Year	N/A	Yearly	Survey year	*In situ* data

ing the observed pattern of whale habitat use off Jan Mayen since water depth is a good predictor of *Hyperoodon ampullatus* distribution in the northeast North Atlantic (Ramírez-Martínez & Hammond 2019) and above the Gully off Nova Scotia (Hooker 1999, Hooker et al. 2002), as well as beaked whale distribution and abundance in the Northeast Atlantic (Rogan et al. 2017). A mean depth–slope interaction term was also included as a predictor variable, as the interaction between depth, slope, and bottlenose whale sightings in the Gully was found to be significant (Hooker 1999, Hooker et al. 2002). The predicted core area for bottlenose whales in the northwestern Atlantic was found to be characterised by aspect (Compton 2004). Distance from the 2000 m depth contour was significantly associated with beaked whale distribution in the northern east Atlantic (Rogan et al. 2017).

The distribution of *Gonatus fabricii* is strongly related to the Norwegian current system. The Norwegian Atlantic current brings *G. fabricii* juveniles northward to waters between Jan Mayen and Vesterålen (Wiborg et al. 1982), while deep-sea adults might join the East Greenland current to reach Jan Mayen (Bjørke 1995). The proximity to the frontal boundary, which appears to be geographically steady across the study period (Raj et al. 2019, Skagseth et al. 2022), is a good predictor of habitat use of beaked whales and squid-feeding sperm whales *Physeter macrocephalus* off the northeastern USA (Waring et al. 2001).

2.4.2. Dynamic environmental variables

Dynamic variables including chl *a* concentration, SST, SSH, and salinity (SA) were included as proxies of cephalopod distribution, given that the squid species, including *Gonatus*, feed on amphipods and copepods (Bjørke 1995). Since chl *a*, SST, and SSH are more likely to reflect plankton growth rather than squid or whale distribution directly (Eppley 1972), 2 mo lagged values (April-averaged) were used to account for the energy transfer across trophic levels. For SA, June-averaged values without a time lag were used, as the distribution of *Gonatus* squid is strongly associated with high SA level (above 35 ppt) in Atlantic waters (Bjørke 1995).

Solar elevation and survey year were also examined to capture any temporal pattern of whale habitat use; the former reflected the effect of hourly change in sun position relative to the horizon, while the latter reflected annual variation between survey years. Elevation angle was calculated based on the algorithm presented by Michalsky (1988) and verified using NOAA's Solar Calculator (Global Radiation Group 2017).

2.5. Bottlenose whale habitat modelling

2.5.1. Detection function analysis

Distance sampling analysis was performed to estimate the detection function for bottlenose whales, using the 'Distance' package v.0.9.6 (Marshall et al. 2016) in R v.3.4.1 (R Core Team 2017). This technique is commonly adopted for distribution and abundance estimates in cetacean studies (Hammond et al. 2002, 2009, 2013, Embling et al. 2010, Rogan et al. 2017). Sightings that involved attraction to the research vessel were excluded from this analysis. Perpendicular distance was re-calculated, followed by truncation of sighting data at a distance to improve model goodness-of-fit while retaining as much data as possible (Buckland et al. 2001). Model fit was examined and compared using QQ plots and goodness-of-fit tests (Buckland et al. 2004).

Conventional distance sampling (CDS) models (Buckland et al. 2001) with half-normal and hazard-rate key functions were fit and compared based on Akaike's information criterion (AIC; Akaike 1992) and QQ plots. The model fits detection probability as a function of perpendicular distance from transect lines. Multi-covariate distance sampling (MCDS) (Marques & Buckland 2003) models were then run to incorporate the potential effects of environmental and sighting conditions in addition to detection distance. Group size and Beaufort sea state were examined to account for covariate-related heterogeneity in detection probability by post-survey stratification of data (Marques & Buckland 2003). Since there were few sightings of group sizes larger than 4 and the environmental conditions at multiple Beaufort scales were similar, some sightings were grouped together for MCDS modelling. CDS and MCDS models with the best functional form (either half-normal or hazard-rate) were examined and compared using AIC and Cramer-von Mises test (i.e. goodness-of-fit test to compare the exact and asymptotic distribution; Cramér 1928), and the best-fitting model was adopted for the estimation of detection probability and associated effective strip width (ESW). Significant effects of group size and/or sea state (if any) would be taken into account in habitat models via the offset, which was calculated as the effort segment length multiplied by twice the ESW.

2.5.2. Sighting occurrence and additional sightings as response variables

Wildlife count data often contain a larger number of zeros (absences of detection) than expected by classical count probability distributions, such as the Poisson distribution. Zero-inflation can be caused by multiple factors, including experimental design, sampling variability, and the size and behaviour of the animal population of interest (Blasco-Moreno et al. 2019). In this study, zero-inflation may have been partly driven by the long dive duration of the study species, which reduces their availability for visual detection at the water surface. Here, the sightings data appeared to be zero-inflated according to Vuong test results (Vuong 1989). A 2-model approach was therefore adopted to accommodate for the zero-inflated nature of sightings data: (1) sighting presence–absence per segment was first modelled with a binomial model for the prediction of occurrence; i.e. expected probability of whale sighting presence–absence, followed by (2) the number of additional whale sightings given first encounter; i.e. zero-truncated counts of sightings conditional on presence, per segment, fitted to a Poisson model. The 2-step model approach (probability function detailed by Zuur et al. 2009 as their Eq. 11.24), also known as the hurdle model developed by Cragg (1971), has been commonly applied in ecological studies aiming to predict relationships between animal sighting data and environmental variables (Agarwal et al. 2002, Barry & Welsh 2002, Potts & Elith 2006, Mellin et al. 2012, Smith et al. 2019). It has also been found to outperform other regression models in terms of model fit between observations and model predictions (Potts & Elith 2006), with flexibility allowing for potential different drivers of animal occurrences and counts. As linear cetacean–habitat relationships are uncommon, sighting presence–absence and additional sightings were fitted with generalised additive models (GAMs; Hastie & Tibshirani 1986) within the 'mgcv' v.1.8-28 (Wood 2016) library in R.

2.5.3. Modelling occurrence of whale sightings

In a first step to understand the effect of each covariate, univariate GAMs were fit within the 'mgcv' library in R to relate sighting presence–absence per segment to each predictor variable. Sighting presence–absence per segment was assumed to follow a Bernoulli distribution, as an animal was either present or absent in a particular effort segment. The expected probability of whale sighting occurrence in the i^{th} segment, $E(y_i)$, is formulated as (Hedley et al. 1999):

$$E(y_i) = g^{-1}(\beta_0 + \Sigma f(z_i)) \quad (1)$$

where $g()$ is the link function, β_0 is the intercept to be estimated, f represents the smooth functions of explanatory covariates, and z_i denotes the value of the explanatory variable in the i^{th} effort segment. A probit link function was chosen for the global binomial model as it has smaller unbiased risk estimator (UBRE) scores in most univariate GAMs. In a similar fashion as AIC, a smaller UBRE score indicates a better model fit (Shadish et al. 2014). Most covariates were included as smooth terms, except for 'year', which was treated as a factor, and the interaction term of mean depth × slope, which was specified as a tensor product interaction allowing covariates to be included at different scales (Wood 2006).

The maximum number of knots (i.e. degrees of freedom, joining successive smoothing splines along the x-axis) was manually set as 8, as the sample size was much larger than 100 (Thomas et al. 2015), and the optimal degree of smoothing was chosen by cross-validation. In addition, covariate terms were specified as thin plate regression splines, whose shrinkage component penalises smooth parameters to zero if no signal is found (Wood 2016). These allow the degrees of freedom to be included as part of the model selection process (Rogan et al. 2017).

Correlation among non-normally distributed covariates was examined by Spearman's rank collinearity test in R (R Core Team 2017). For highly correlated variables ($r > 0.5$ or $r < -0.5$), only the one that explained more of the deviance, with a lower UBRE score, and was more informative and ecologically influential (i.e. with more direct ecological impacts) was retained based on the univariate model results. This selection process improves model reliability by ensuring that the assumption of independence among explanatory variables is not violated (Thomas et al. 2015). Selected covariates from the univariate models were included in a global multivariable model for the occurrence model selection.

2.5.4. Binomial model selection and model-averaged predictions

Since GAMs with different degrees of smoothness are not nested, global model selection rather than stepwise selection was performed within the 'MuMIn' (Bartoń 2015) library in R. The smooth

terms of latitude and longitude were excluded as candidate covariates prior to model selection, given that the spatial coverage of the surveyed area was uneven in terms of coordinates, and model estimates for a wider prediction area would thus be highly uncertain. Models with all other possible covariate combinations were compared by small-sample corrected AIC (AICc) (Cavanaugh 1997) and model weight. Model fit was also examined by UBRE score, adjusted R^2 value (reflecting the proportion of variance explained), and the percentage of deviance explained by the model.

Standard model diagnostics tests (residual plots, influence, and leverage plots) were then performed for the best binomial GAM, although the binary nature of the response variable makes residual plots (except for QQ plots) difficult to interpret. Serial residual correlation was checked using the Durbin-Watson test (Durbin & Watson 1971) and illustrated by autocorrelation function (ACF) plot (Fox et al. 2016) after model selection, as it could not be incorporated into the GAM together with the shrinkage smooth terms. A particular time lag with $p < 0.05$ in the Durbin-Watson test or with an ACF score exceeding the threshold values for statistical significance (illustrated as horizontal dotted lines in the ACF plot) was considered to imply serial correlation (Thomas et al. 2015).

Uncertainty in model selection due to the large number of covariate combinations was addressed by model averaging (Burnham & Anderson 2002), in which spatial prediction was made based on a confidence set of models with $\Delta AICc < 2$. Model-averaged predictions of sighting occurrence and associated coefficients of variation (CVs) were calculated for each prediction grid. The relative importance of each predictor variable was calculated by the summation of Akaike weights. Model-averaged predictions of sighting occurrence were then plotted throughout the range of each significant covariate (with $\alpha = 0.05$), given that other predictor variables were fixed at their mean values.

2.5.5. Modelling the number of additional whale sightings given a first encounter

Similar to the GAM for sighting occurrence, the respective relationships between the number of additional sightings per segment (provided there was at least one sighting) and each predictor variable were first modelled as univariate GAMs. This approach is designed to independently model additional whale sightings given a first encounter as a response parameter, which is not accounted for in the occurrence-only model. The response variable was assumed to follow a Poisson distribution, which required the estimation of a single rate parameter, λ. The expected number of additional whale sightings in the i^{th} segment, $E(x_i)$, can also be calculated by Eq. (1), except that a log link function was specified due to its lower UBRE score. An interaction term between mean depth and slope was also included. The maximum degrees of freedom were set manually, and over-fitting was prevented in the same way as for the occurrence model. Model selection and diagnostics were carried out following the same criteria and procedures as for the occurrence model, with the same covariate set as suggested by univariate models, and a covariate collinearity test being specified in the global Poisson GAM. Model-averaged predictions of the number of additional whale sightings given a first encounter, CV, and covariate effects were estimated and visualised in the same way as the occurrence predictions. It should be noted that group size of whale sighting was not included in the Poisson GAM, as it is potentially correlated with social factors other than environmental variables, e.g. male bottlenose whales appeared to form stronger associations with con-specifics in their own age classes compared with females and immature individuals (Gowans et al. 2001).

2.5.6. Zero-inflated Poisson location-scale model

The 2-model estimates of habitat-use relationships were validated by a zero-inflated Poisson location-scale model within the 'mgcv' library in R. The zero-inflated GAM consists of 2 linear predictors: one controls the probability of occurrence with a logit link function, while the other controls the Poisson parameter given first encounter with a log link function (Wood 2016). The first and second formulae of the model specify the multivariate response and the linear predictor structure respectively for Poisson and binomial parameters (Wood 2016). Here, the response variable was simply the number of whale sightings made per segment. Covariate sets for the best models of additional sightings given a first encounter and sighting occurrence were specified in the first and second formulae respectively. Given comparable model assumptions such as $\alpha = 0.05$, model estimates of the zero-inflated GAM were expected to be similar to those of the 2-model hurdle approach.

2.5.7. Spatial prediction of habitat use

The predicted pattern of habitat use in relation to the environmental covariates for a wider area (Fig. 1) was obtained by quantifying environmental covariates retained in our near Jan Mayen habitat model. Model-averaged estimates of sighting occurrence and number of additional whale sightings + 1 were multiplied (i.e. occurrence probability × sightings, so as to calculate the predicted total number of whale sighting for each grid with the observed number of sightings) for each prediction grid. Standard error (SE) was first calculated as the square root of the sum of estimated variances of occurrence and additional sightings given a first encounter (Buckland et al. 2001), and it was then converted to CV as a measure of prediction uncertainty.

3. RESULTS

A total of about 4000 km of survey distance was included in the analysis, with a roughly equal distribution of effort across the 3 yr (2014–2016). Northern bottlenose whales were regularly sighted in the surveyed area each year, with a mean survey distance per sighting of approximately 18 km (Table 1). The average group size of sightings was 3.1 ± 1.4 whales, resulting in a mean survey distance per individual of 5.8 km off Jan Mayen Island, compared to 1463.9 km in Norway and 104.6 km in Iceland-Faroes as per Ramírez-Martínez & Hammond (2019).

3.1. Detection function analysis

A total of 26 of 220 sightings were scored in the field as whales being attracted to the research vessel (labelled as 'strong seekers' as part of the field data collection) and were discarded prior to detection function modelling. The truncation distance was set to 700 m, retaining approximately 167 sightings, which was ~85% of non-seeking sightings. The final best model for detection probability was a hazard-rate CDS model as a function of perpendicular distance (Fig. 2), followed by MCDS models all with ΔAIC > 2 (Table 3). The average detection probability of bottlenose whales given the 700 m truncation distance was estimated to be 0.33 (CV = 0.15), for an effective half-strip width of 231 m or ESW of 462 m. The 0.33 correction factor was applied to all effort segments assuming that the survey years and whole surveyed area was homogenous in terms of detection probability. No offset or ESW information was fitted to habitat models for occurrence and additional sighting estimates.

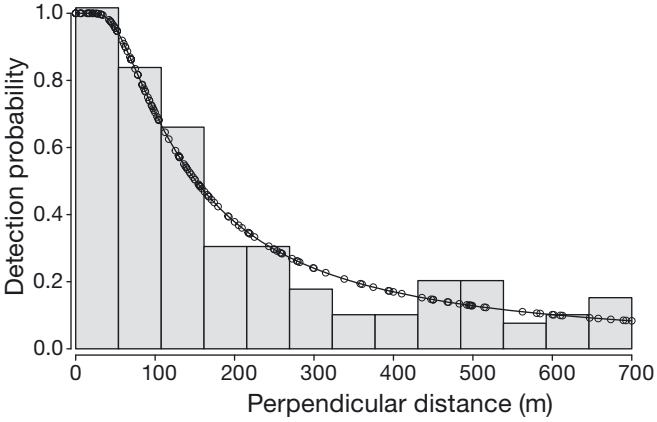

Fig. 2. Detection function fit for the hazard-rate conventional distance sampling model with a truncation distance of 700 m. Open circles: perpendicular distances of sightings of northern bottlenose whales; smoothed curve: the fitted detection function

3.2. Habitat modelling

Based on the results of the covariate collinearity test and univariate modelling of both response variables (sighting presence–absence and additional sightings), global models with 7 covariates (including mean depth, distance from Arctic front, April chlorophyll concentration, April SST, slope, solar elevation, and aspect) and the tensor product term of depth–slope interaction were established for model selection.

3.2.1. Occurrence of whale sightings

The best occurrence model (with the lowest UBRE score and AIC) retained bathymetric slope, April chlorophyll concentration, April SST, and a topographic interaction of depth with slope, explaining 8.4% of the deviance (Table 4). With the first 2 variables also gaining statistical support ($p < 0.05$) in the zero-inflated Poisson location-scale model, sighting occurrence was found to increase with steeper topography (Fig. 3a) and was correlated with lower April concentration of chlorophyll (below 0.4 mg m^{-3}), with greater prediction uncertainty above 1 mg m^{-3} (Fig. 3b). SST became insignificant ($p > 0.05$) when the same covariate set was specified in the zero-inflated Poisson GAM, indicating that the effect of SST

Table 3. Detection function models for northern bottlenose whales. Models are sorted in ascending order of Akaike's information criterion (AIC); hr.model was the final best model. hr: hazard-rate key function; n: size; ss: Beaufort sea state; hn: half-normal key function; as.factor() indicates the conversion of integer variable to categorical variable; CV: coefficient of variation

	Key function	Formula	AIC	Cramer-von Mises p-value	Average detectability	SE	CV	ΔAIC
hr.model	hr	~1	2088	0.79	0.326	0.047	0.15	0
hr.n.model	hr	~as.factor(grouped_size)	2094.3	0.84	0.336	0.048	0.14	6.3
hr.ss.model	hr	~as.factor(grouped_beaufort)	2094.6	0.88	0.305	0.048	0.16	6.6
hr.ss.n.model	hr	~as.factor(grouped_beaufort) + as.factor(grouped_size)	2100.7	0.91	0.316	0.048	0.15	12.7
hn.model	hn	~1	2114.7	0	0.51	0.025	0.05	26.7

Table 4. Best models of sighting occurrence and number of additional sightings, given a first encounter of a northern bottlenose whale. MaxK: maximum number of knots allowed; edf: estimated degree of freedom, %DevEx: % deviance explained; UBRE: unbiased risk estimator; AIC: Akaike's information criterion. See Table 2 for covariate descriptions

	Covariates	MaxK	edf	p ($\alpha = 0.05$)	%DevEx	UBRE	AIC	Model weight
Best sighting occurrence model	slope.max	4	0.798	0.038	8.44	0.2438	393.1	0.03
	April Chla	4	1.84	0.028				
	August SST	4	2.902	0.010				
	depth.m:slope.max	5	0.807	0.178				
Best additional sightings model	depth.m:slope.max	8	3.68	0.001	23.4	0.1899	258.129	0.036
	distAF	4	2.15	0.015				
	April Chla	6	1.93	0.111				
	August SST	5	0	0.472				
	depth.m	4	0	0.704				
	slope.max	6	0	0.895				
	aspect	6	0	0.944				

was not robust. The model was interpreted without incorporating any autoregressive structure (AR[1] or ARIMA), given that general additive mixed models (GAMMs; Chen 2000) are reported to perform poorly with binary data (Wood 2016). Nevertheless, it should be noted that SE, confidence intervals (CIs), and CVs quantifying the uncertainty in covariate effects were likely to have been somewhat underestimated without incorporating any autoregressive structure. Occurrence model diagnostics are detailed in the Supplement at www.int-res.com/articles/suppl/m718p119_supp.pdf.

3.2.2. Average estimates of occurrence based on the confidence set of models

The confidence set consisted of 49 models with ΔAICc < 2, which accounted for 70.4% of total Akaike weights. SST in April and chlorophyll concentration in April were respectively the most and second most important variables with high relative importance (with summed Akaike weights of 1 and 0.95, respectively) and were included in nearly all models among the confidence set. Maximum slope was moderately important (with a relative importance of 0.67) and was retained in about 60% of all models among the confidence set.

Model-averaged predictions of occurrence plotted against each statistically supported covariate, with other explanatory variables fixed at their mean values in the data, are given in Fig. 3. Similar to the best occurrence model estimates, higher occurrence was predicted at steeper topography (Fig. 3c) and April chlorophyll concentration below 0.4 and above 1 mg m^{-3}, with greater prediction uncertainty above 1 mg m^{-3} (Fig. 3d). Spatial estimates of sighting occurrence were based on model-averaged predictions and are further detailed in the Supplement.

3.2.3. Number of additional whale sightings given a first encounter: GAM results

The number of additional whale sightings given a first encounter (total number of whale sightings – 1)

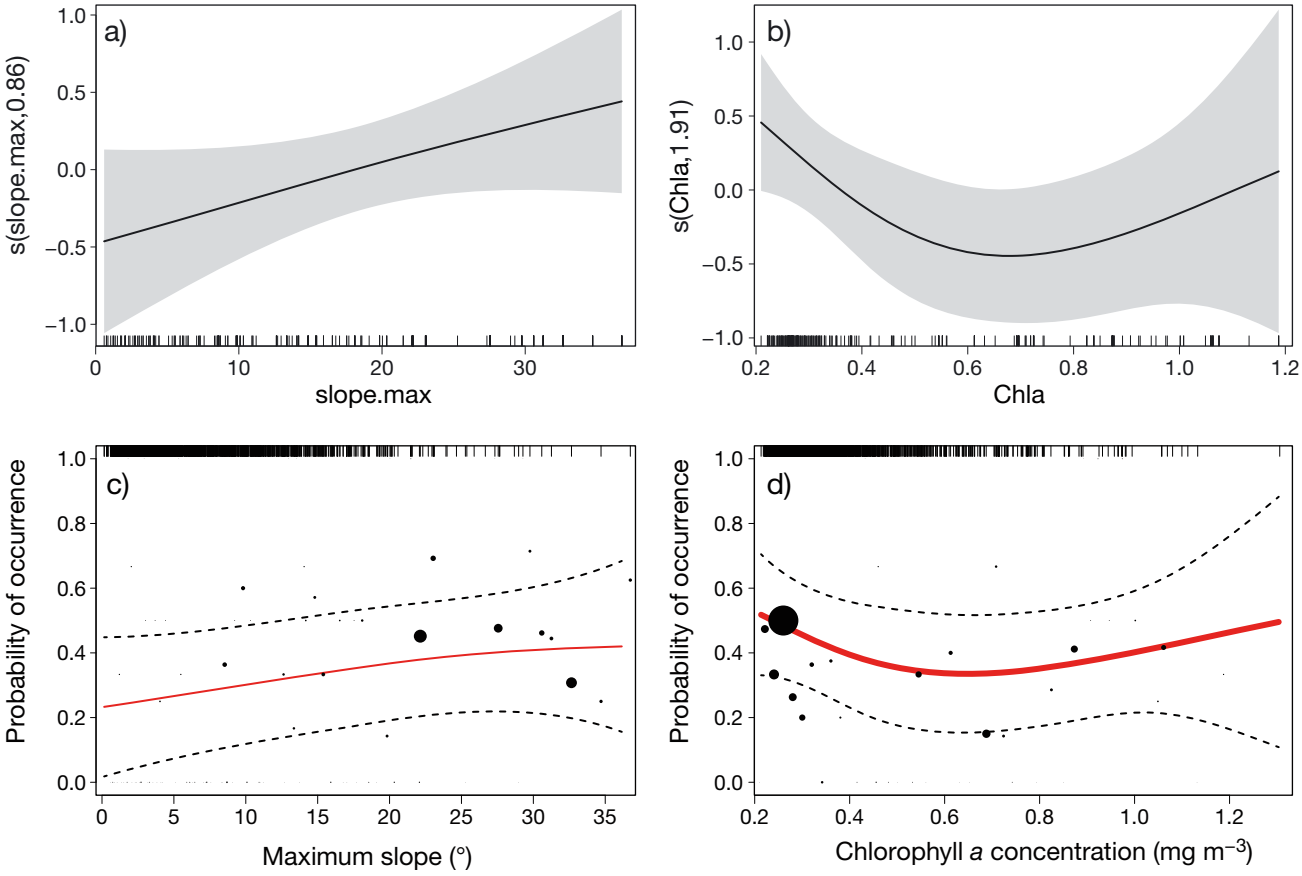

Fig. 3. Component smooth functions of (a) maximum slope (in degrees); and (b) April chlorophyll concentration (in mg m^{-3}). Model-averaged estimates (red curves) of northern bottlenose whale occurrence probability as a function of (c) slope and (d) April chlorophyll concentration throughout environmental predictor ranges, given the mean values of other covariates. Solid lines: smooth estimates; shaded bands in (a) and (b) and dash lines in (c) and (d): ±2 SE. Dots in (c) and (d): original data; dot size is proportional to the sample size within the defined bins

was modelled as a function of the same covariate set (see Section 4.2) in the global Poisson GAM. The final best Poisson model with the lowest UBRE score and AIC retained all covariates except for solar elevation, while the 6 explanatory variables and one topographic interaction term together explained 23.4% of the deviance (Table 4). With depth–slope tensor product term also being the only statistically supported variable at the 5% level in the zero-inflated Poisson GAM, the number of additional whale sightings given a first encounter at different water depths appeared to depend on seafloor slope: steep topography increased the expected additional number of whale sightings given a first encounter at shallower water depths (<750 m), while more whale sightings were estimated in deep waters (about 2000 m) with gentle slopes (Fig. 4). Distance from the Arctic front lost statistical support ($p > 0.05$) when the variable was specified in the zero-inflated Poisson GAM, indicating that the effect of this predictor was not robust. As a GAMM could not effectively correct for serial correlation in this case, the best additional sightings model was also interpreted without any autoregressive structure. SEs, CIs, and CVs were also likely to have been underestimated under serial correlation. Model diagnostics for the Poisson GAM are further explained in the Supplement.

3.2.4. Average estimates of the number of additional whale sightings given a first encounter: confidence set of models

The confidence set included 25 models with ΔAICc < 2, accounting for 61.7% of total Akaike weights. The depth–slope interaction term, distance from Arctic front, and depth were the 3 most important variables, and they were retained in almost all models

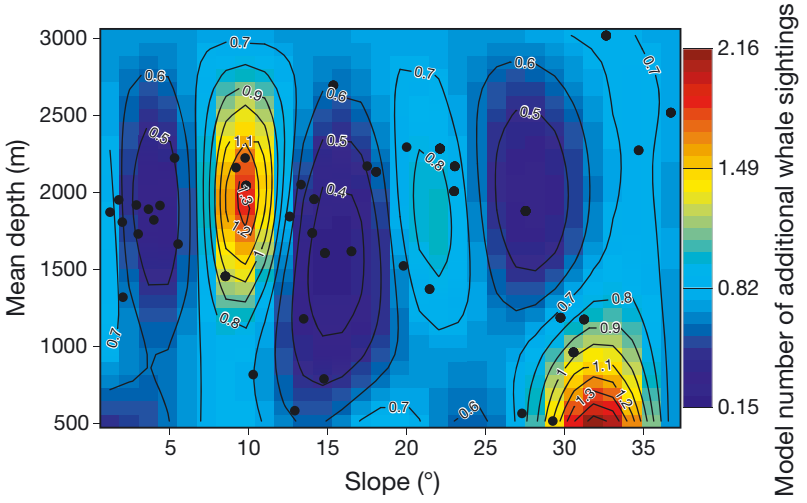

Fig. 4. Modelled values of additional northern bottlenose whale sightings given a first encounter on the response scale, as a function of the interaction between mean depth and slope. Black points: whale-present observations

among the confidence set with very high relative importance (Akaike weight ~ 1).

Model-averaged predictions of additional whale sightings given a first encounter were plotted throughout the range of each important covariate in Fig. 5. The effect plot for the tensor interaction term between mean depth and slope (Fig. 5a) illustrated that more bottlenose whales were estimated at water depths between 1000 and 2500 m with flat topography, whereas those found at water depths shallower than 1000 m preferred steeper seafloor slope. The SE values of model predictions made for shallow water depths with steep slopes were high, given that the estimates were dominated by few data points (Fig. 5b).

3.2.5. Wider area habitat use prediction

The predicted pattern of potential habitat use based on estimates of sighting occurrence multiplied by the estimated number of total whale sightings (additional number of whale sightings given a first encounter + 1) was concordant with whale sightings recorded in the surveyed area along the West Jan Mayen Fracture Zone: higher sighting rates were predicted in the southeast of the submarine canyon and off Jan Mayen Island (Fig. 6). Higher numbers of whale sightings were predicted in areas northwest of Jan Mayen Island, which were similar to the occurrence model estimates. Fewer sightings were predicted in the southeast corner of the wider prediction area and coastal waters south of Jan Mayen, which was consistent with the spatial estimates of the whale sighting occurrence model. Higher prediction uncertainty (i.e. higher CV) was estimated in the southeast corner of the wider prediction area, matching the lower survey effort in the area.

4. DISCUSSION

Regular bottlenose whale sightings were made yearly during the survey efforts in June 2014–2016, indicating an overall high level of use of the surveyed area at those times. The average group size sighted

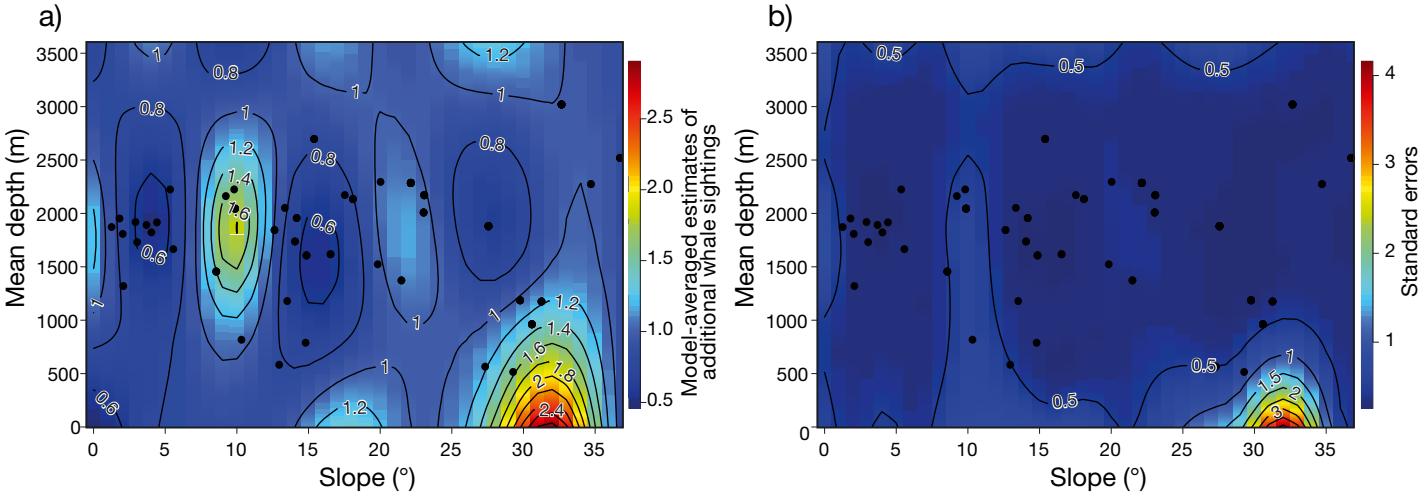

Fig. 5. (a) Model-averaged estimates of additional northern bottlenose whale sightings given first encounter as a function of the depth-slope interaction term and (b) associated SE values. Black points: whale-present observations

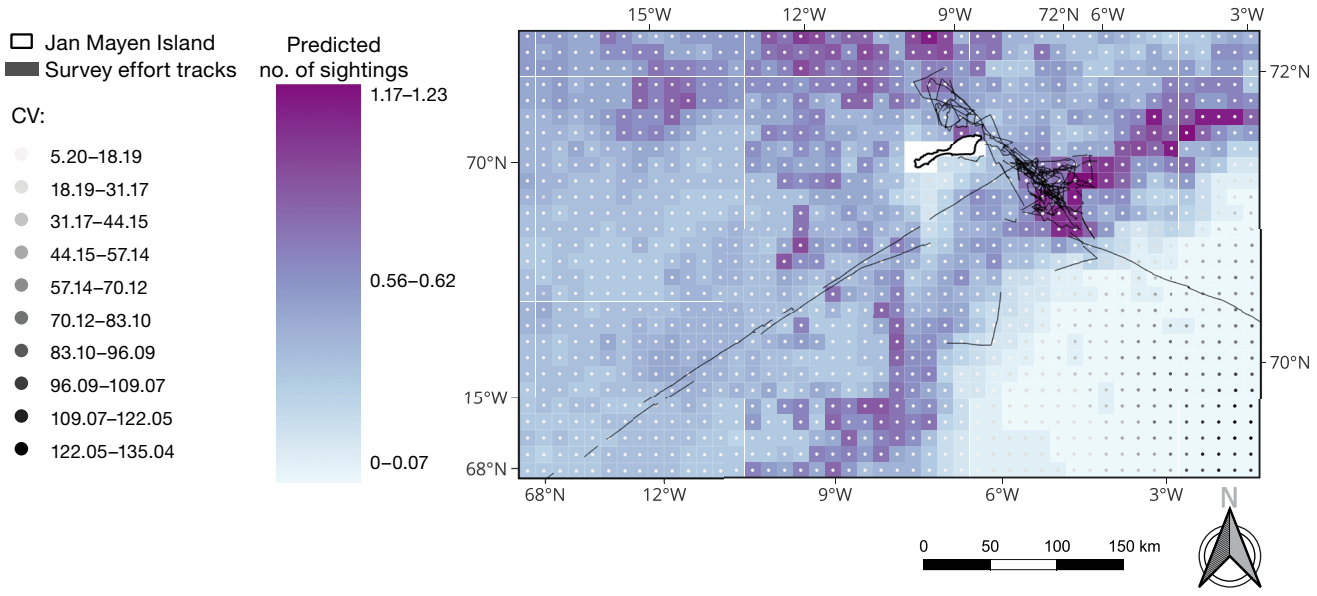

Fig. 6. Spatial estimates of the number of northern bottlenose whale sightings over the wider prediction area, based upon the observed pattern of sightings in the smaller surveyed area covered by effort tracks. Model estimates are illustrated by the colour of grid cells. The associated coefficient of variation (CV) is represented by the centroid point, with higher CV values indicated by darker dot colour

was about 3 individuals, which was consistent with the group sizes observed near Jan Mayen in June 2013 (Miller et al. 2015b), although some larger group sizes were noted by Ramírez-Martínez & Hammond (2019, see their Fig. 22). While the sighting platform used in this study was likely less effective than the shipboard double-platform of the study by Ramírez-Martínez & Hammond (2019), the ESWs for both studies were similar (N. C. Ramírez-Martínez pers. comm.). The much shorter mean survey distance per animal in our study (6 km whale^{-1}; Table 1) versus that of the wider regions covered by Ramírez-Martínez & Hammond (2019) (105–1460 km whale^{-1}; see their Table 2) therefore indicates that a relatively high sighting rate of northern bottlenose whales occurred in Jan Mayen in the period surveyed.

4.1. Species–habitat modelling

4.1.1. Model estimates and significant environmental correlates

Binomial model results indicated that seafloor slope and April chlorophyll concentration were significant correlates of bottlenose whale sighting occurrence within the wider prediction area during June 2014–2016. Preference for steep bathymetry (Fig. 3c) around Jan Mayen Island is consistent with bottlenose whale habitat preference off eastern Canada: higher whale encounter rate (i.e. the number of encounters divided by number of hours of effort) was correlated with steeper seafloor slope within the Gully submarine canyon (Hooker et al. 2002). The estimated relationship may be driven by the ontogenetic descent in juvenile *Gonatus*, which perform vertical migration from shallow water to depths over 1000 m upon maturity (Hooker 1999, Bjørke 2001). This could attract whales to deeper water in order to feed on prey of greater body sizes. The probability of whale sighting was also found to be higher in concentrations of chlorophyll below 0.4 mg m^{-3} in April (Fig. 3d), which was also predicted in the zero-inflated Poisson GAM. This pattern is different from the chlorophyll relationship typically observed in other cetacean species: animal distribution positively correlates with productive waters with higher sea surface chlorophyll concentrations (Smith et al. 1986, Redfern et al. 2008), an indirect indication of high prey abundance. However, a negative correlation between chlorophyll concentration in April and bottlenose whale density across the broader northeast Atlantic over summer periods from 1998 to 2015 was also identified by Ramírez-Martínez & Hammond (2019, their Fig. 25). This result may be explained by the incorporation of the 2 mo temporal lag, which might not be effective in capturing the spatial disconnect between surface productivity and deep-water prey abundance, and/or the effect of chlorophyll concentration on prey abundance. Alternatively, there

could potentially be other, unexplored environmental variable(s) that would better explain the observed negative relationship ecologically. We suggest that future research is needed to obtain field data with longer temporal coverage and further explore the effects of other environmental variables on bottlenose whale occurrence or density.

The Poisson GAM showed that depth–slope interactions and whale distance from the Arctic front were significant predictors of additional whale sightings given a first encounter. However, distance from the Arctic front did not gain statistical support when it was specified in the zero-inflated Poisson GAM, indicating that the effect identified in the Poisson GAM was not robust. More whale sightings in water depths between 1000 and 2500 m (Fig. 5a) was consistent with findings in the literature; bottlenose whales in the Gully and northeast Atlantic waters are mainly found in offshore waters deeper than 500 m (Benjaminsen 1972, Benjaminsen & Christensen 1979, Hooker 1999, Rogan et al. 2017, Ramírez-Martínez et al. 2019, Whitehead et al. 2021). Reliance on submarine canyons by the Gully population might even cause it to be genetically different from individuals in the rest of eastern Canada (Feyrer 2021), as whales around the Labrador-Davis Strait are more evenly distributed along the continental shelf edge and in deep basins (Reeves et al.1993, Gomez et al. 2017, Feyrer 2021). Preference for deeper water could be driven by the downward vertical migration in maturing prey *Gonatus* (Hooker 1999, Bjørke 2001). Although some whales were sighted at shallower water depths (<500 m) in the field, the predicted effect of the interaction term between mean depth and slope revealed that steep seafloor topography (and thus deeper water) was located nearby.

Despite the unclear effect of seasonal migration (Benjaminsen & Christensen 1979, Reeves et al. 1993) on the habitat use of bottlenose whales in the northeast Atlantic, the potential migration patterns might be one of the reasons for the low percentages of deviance explained by the best models of sighting occurrence and additional whale sightings given a first encounter in this study. Whaling records in Norway suggested that bottlenose whales might reach their northern distribution in spring and early summer and migrate southward in July (Reeves et al. 1993). The north–south migration hypothesis is further supported by Miller et al. (2015b), who tagged whales off Jan Mayen Island in June 2015. The tagged individuals exhibited southward directional movements, with one travelling long distances to the Azores Archipelago between late June and early August 2015. Whale strandings along Europe and Ireland, peaking in late summer and autumn, suggest northward whale movement in spring and later southward movement between late summer and autumn (Whitehead & Hooker 2012). Year-round records of bottlenose whales off the Faroe Islands (Bloch et al. 1996) and Norway (Øien & Hartvedt 2011) suggest that bottlenose whales in the northeast North Atlantic might exhibit inshore–offshore movement driven by the seasonal change of prey abundance (Whitehead & Hooker 2012). In this study, some whale sightings were recorded during the vessel transit between Jan Mayen Island and Iceland (Fig. 1), which could have been whales migrating southward or offshore.

4.1.2. Spatial prediction of whale habitat use over the wider prediction area

Spatial predictions of whale habitat use over a wider area using the 2-model approach (Fig. 6) corresponded to field observations of this study: *in situ* bottlenose whale sightings were mostly made to the east of Jan Mayen Island and the submarine canyon southeast of Jan Mayen. They also indicated that the submarine canyon area to the southeast of Jan Mayen Island (marine region ranging from 70.8° N, 6.5° W to 71.2° N, 5.5° W) could be a high-use site by bottlenose whales in summer. These estimates were largely consistent with the model predictions of both the binomial and Poisson GAMs of this study, and average density prediction for bottlenose whales from 1998 to 2005 for the broader northeast North Atlantic by Ramírez-Martínez & Hammond (2019, see their Fig. 26).

An apparent preference for submarine canyon habitats has been observed in bottlenose whales, sperm whales, and striped dolphins *Stenella coeruleoalba* in the Gully off Nova Scotia, and sperm whales within the Andøya Canyon northwest of Andenes, Norway (Teloni et al. 2008). Submarine canyons are often regarded as biomass and biodiversity hotspots (Vetter & Dayton 1999, De Leo et al. 2010, Amaro et al. 2016) that are capable of sustaining ecologically complex communities. These topographic features act as conduits for the influx of macrophyte detritus and diel vertical migrators which are later distributed throughout much of the canyon system by strong gravity currents (Greene et al. 1988, Vetter & Dayton 1999). Canyon hydrographic effects such as accelerated currents enhance the concentration of suspended particulate matter (De Leo et al.2010). Organic matter together with strong

habitat heterogeneity within canyons substantially support a diversity and abundance of benthic fauna, including mega-benthic invertebrates (De Leo et al. 2010, Santo 2010) and deep-sea fish (Vetter & Dayton 1999). Epibenthic diversity within the Jan Mayen Fracture Zone (and the submarine canyon) is relatively high, in which Oschmann (1991) identified 36 taxa and Santo (2010) found 47 identifiable species among 66 disparate species (including crinoideans, anthozoans, tunicates, poriferans, fishes, and hexacorallian corals). Eurybathic species appear to be remarkably abundant between 580 and 3222 m (Oschmann 1991). This might favour the underwater aggregation of adult *Gonatus* squid at 1000 m or below or other prey and, in turn, attract bottlenose whales to forage within the canyon area.

Although higher sighting rates were also estimated in waters from 71.3° N, 4.5° W to 71.8° N, 1.5° W, northern and northwestern waters off Jan Mayen Island, as well as waters south of the study region (similar southern Jan Mayen pattern was also predicted by Ramírez-Martínez & Hammond 2019), model estimates of these areas should be treated carefully, as at-field whale observations or dedicated survey effort did not cover these areas.

In addition, the 2-model approach alias hurdle model can only deal with excessive zeros by modelling additional whale sightings given a first encounter with a zero-truncated Poisson distribution, but not differentiate true zeros (i.e. actual absence of an animals) from false zeros (i.e. animal is present but detected). As some false zeros might potentially arise from availability or perception bias, these model predictions should be corroborated by systematic and ideally year-round line-transect studies incorporating both visual and acoustic detection. Such monitoring would help to equally sample the whole survey area, while survey bias on detection probability can be minimised. By reducing false zeros and model prediction uncertainty, this can potentially inform the delineation of marine protected area(s) covering important whale habitat in Jan Mayen waters for effective conservation of bottlenose whales in the northeast North Atlantic.

4.2. Conservation insights of northern bottlenose whales off Jan Mayen Island

Our study indicates a potential key habitat for northern bottlenose whales around Jan Mayen in June, particularly the submarine canyon area to the southeast of the island. This potential high-use site is not currently under any statutory protection, such as the Jan Mayen Nature Reserve designated in 2010, which covers a total area of 4315 km^2 of Jan Mayen territorial waters (up to 22.2 km from the island; Bruserud et al. 2010).

In the meantime, oil and gas surveys using airguns have been frequent along the coast of Norway (see www.npd.no/en). The Norwegian government recently proposed opening its waters to deep-sea mining (see https://www.reuters.com/sustainability/climate-energy/norway-moves-open-its-waters-deep-sea-mining-2023-06-20). A recent study has documented the effects of airgun sounds on narwhals *Monodon monoceros* (Heide-Jørgensen et al. 2021), another marine mammal species living in high-latitude regions. Though northern bottlenose whales can display strong inquisitiveness to unfamiliar sounds (Hooker 1999, Miller et al. 2015a), acoustic disturbance is regarded as one of the key threats to this beaked whale species (Whitehead et al. 2021). Beaked whales may be more behaviourally responsive to man-made noise in relatively pristine waters such as around Jan Mayen compared to areas with frequent human activity (Wensveen et al. 2019). Northern bottlenose whales were found to exhibit strong behavioural responses with relatively low response thresholds to sonar signals, with long-term area avoidance and cessation of echolocation-based foraging (Miller et al. 2015a, Sivle et al. 2015, Wensveen et al. 2019) indicating consequent risk from marine development and naval activity. Along with these previous studies, the findings here can, to a certain extent, inform the management of underwater noise threats by minimising spatial overlap between potential high-use areas of bottlenose whales and future noise-generating anthropogenic activities, such as seismic surveys.

Data accessibility. Original whale sightings data are available from Dryad at https://doi.org/10.5061/dryad.wm37pvmt5

Acknowledgements. We express our sincere gratitude to everyone involved in the Jan Mayen fieldwork, including Captains Christian Harboe-Hansen and Chris Rose and the rest of the ship's crews. Thanks to the science crews including Tomoko Narazaki, Kagari Aoki, Leigh Hickmott, Lucia Martina Martin Lopez, Lars Kleivane, Rune Hansen, Miguel Neves dos Reis, Dr. Eilidh Siegal, Paul Wensveen, Eva Hartvig, Mike Williamson, Naomi Boon, Joanna Kershaw, Hannah Wood, Eva Hartvig, and Charlotte Curé. Invaluable scientific and/or editorial advice was provided by Prof. Phil Hammond, Nadya Ramírez-Martínez, Guilherme Augusto Bortolotto, the editor, and anonymous reviewers to improve the quality of the manuscript. This project was primarily funded by SERDP project RC-2337 and the US Office of Naval Research.

LITERATURE CITED

Agarwal DK, Gelfand AE, Citron-Pousty S (2002) Zero-inflated models with application to spatial count data. Environ Ecol Stat 9:341–355

Akaike H (1992) Information theory and an extension of the maximum likelihood principle. In: Parzen E, Tanabe K, Kitagawa G (eds) Selected papers of Hirotugu Akaike. Springer Series in Statistics. Springer, New York, NY, p 199–213

Amaro T, Huvenne VAI, Allcock AL, Aslam T and others (2016) The Whittard Canyon — a case study of submarine canyon processes. Prog Oceanogr 146:38–57

Barry SC, Welsh AH (2002) Generalized additive modelling and zero inflated count data. Ecol Modell 157:179–188

Bartoń K (2015) MuMIn: multi-model inference. R package version 1.15.6. https://cran.r-project.org/web/packages/MuMIn/index.html (accessed 25 Jan 2017)

Benjaminsen T (1972) On the biology of the bottlenose whale, *Hyperoodon ampullatus* (Forster). Nor J Zool 20: 233–241

Benjaminsen T, Christensen I (1979) The natural history of bottlenose whales, *Hyperoodon ampullatus*. In: Winn HE, Olla BL (eds) Behaviour of marine mammals: current perspectives in research. Plenum Press, New York, NY, p 143–164

Bjørke H (2001) Predators of the squid *Gonatus fabricii* (Lichtenstein) in the Norwegian Sea. Fish Res 52: 113–120

Bjørke H (1995) Norwegian investigations on *Gonatus fabricii* (Lichtenstein). https://hdl.handle.net/11250/105443 (accessed 25 Jan 2017)

Blasco-Moreno A, Pérez-Casany M, Puig P, Morante M, Castells E (2019) What does a zero mean? Understanding false, random and structural zeros in ecology. Methods Ecol Evol 10:949–959

Bloch D, Desportes G, Zachariassen M, Christensen I (1996) The northern bottlenose whale in the Faroe Islands, 1584–1993. J Zool 239:123–140

BODC (British Oceanographic Data Centre) (2003) General Bathymetric Chart of the Oceans (GEBCO). https://www.bodc.ac.uk/data/hosted_data_systems/gebco_gridded_bathymetry_data/

Børsheim KY, Milutinovi S, Drinkwater KF (2014) TOC and satellite-sensed chlorophyll and primary production at the Arctic Front in the Nordic Seas. J Mar Syst 139: 373–382

Bruserud H, Grimstad K, Høyland TK, Stokkan BE, Egeland LC (2010) Forskrift om fredning av Jan Mayen naturreservat. https://lovdata.no/dokument/SF/forskrift/2010-11-19-1456 (accessed 4 Nov 2019)

Buckland ST, Anderson DR, Burnham KP, Laake JL, Borchers DL, Thomas L (2001) Introduction to distance sampling: estimating abundance of biological populations. Oxford University Press, Oxford

Buckland ST, Anderson DR, Burnham KP, Borchers DL, Thomas L (2004) Advanced distance sampling: estimating abundance of biological populations. Oxford University Press, Oxford

Burnham KP, Anderson DR (2002) Model selection and multimodel inference: a practical information–theoretic approach. Springer, New York, NY

Cañadas A, Sagarminaga R, De Stephanis R, Urquiola E, Hammond PS (2005) Habitat preference modelling as a conservation tool: proposals for marine protected areas for cetaceans in southern Spanish waters. Aquat Conserv 15:495–521

Cavanaugh JE (1997) Unifying the derivations for the Akaike and corrected Akaike information criteria. Stat Probab Lett 33:201–208

Chen C (2000) Generalized additive mixed models. Commun Stat Theory Methods 29:1257–1271

Compton RC (2004) Predicting key habitat and potential distribution of northern bottlenose whales (*Hyperoodon ampullatus*) in the northwest Atlantic Ocean. MSc dissertation, University of Plymouth

COSEWIC (Committee on the Status of Endangered Wildlife in Canada) (2011) COSEWIC assessment and status report on the northern bottlenose whale *Hyperoodon ampullatus* in Canada. Committee on the Status of Endangered Wildlife in Canada, Ottawa

Cragg JG (1971) Some statistical models for limited dependent variables with application to the demand for durable goods. Econometrica 39:829–844

Cramér H (1928) On the composition of elementary errors. Scand Actuar J 1928:13–74

de Greef E, Einfeldt AL, Miller PJO, Ferguson SH and others (2022) Genomics reveal population structure, evolutionary history, and signatures of selection in the northern bottlenose whale, *Hyperoodon ampullatus*. Mol Ecol 31: 4919–4931

De Leo FC, Smith CR, Rowden AA, Bowden DA, Clark MR (2010) Submarine canyons: hotspots of benthic biomass and productivity in the deep sea. Proc R Soc B 277: 2783–2792

De Schepper S, Schreck M, Beck KM, Matthiessen J, Fahl K, Mangerud G (2015) Early Pliocene onset of modern Nordic Seas circulation related to ocean gateway changes. Nat Commun 6:8659

Durbin J, Watson GS (1971) Testing for serial correlation in least squares regression. III. Biometrika 58:1–19

Einfeldt A, Feyrer LJ, Paterson I, Ferguson S, Miller P, de Greef E, Bentzen P (2022) Characterization of population structure in northern bottlenose whales (*Hyperoodon ampullatus*) in the North Atlantic from an analysis of microsatellite data. Can Tech Rep Fish Aquat Sci 3467: 1–17

Embling CB, Gillibrand PA, Gordon J, Shrimpton J, Stevick PT, Hammond PS (2010) Using habitat models to identify suitable sites for marine protected areas for harbour porpoises (*Phocoena phocoena*). Biol Conserv 143:267–279

Eppley RW (1972) Temperature and phytoplankton growth in the sea. Fish Bull 70:1063–1085

Erga SR, Ssebiyonga N, Hamre B, Frette O and others (2014) Environmental control of phytoplankton distribution and photosynthetic performance at the Jan Mayen Front in the Norwegian Sea. J Mar Syst 130:193–205

Fernández R, Pierce GJ, MacLeod CD, Brownlow A and others (2014) Strandings of northern bottlenose whales, *Hyperoodon ampullatus*, in the north-east Atlantic: seasonality and diet. J Mar Biol Assoc UK 94:1109–1116

Feyrer LJ (2021) Northern bottlenose whales in Canada: the story of exploitation, conservation and recovery. PhD dissertation, Dalhousie University, Halifax

Feyrer LJ, Zhao ST, Whitehead H, Matthews CJD (2020) Prolonged maternal investment in northern bottlenose whales alters our understanding of beaked whale reproductive life history. PLOS ONE 15:e0235114

Forney KA (2000) Environmental models of cetacean abun-

dance: reducing uncertainty in population trends. Conserv Biol 14:1271–1286

Fox J, Weisberg S, Adler D, Bates D and others (2016) car: companion to applied regression. https://cran.r-project.org/web/packages/car/index.html (accessed 27 Jan 2017)

Glennie R, Buckland ST, Thomas L (2015) The effect of animal movement on line transect estimates of abundance. PLOS ONE 10:e0121333

Global Radiation Group (2017) NOAA solar calculator. https://www.esrl.noaa.gov/gmd/grad/solcalc/

Gomez C, Lawson J, Kouwenberg AL, Moors-Murphy H and others (2017) Predicted distribution of whales at risk: identifying priority areas to enhance cetacean monitoring in the Northwest Atlantic Ocean. Endang Species Res 32:437–458

Gowans S, Whitehead H, Arch JK, Hooker SK (2000) Population size and residency patterns of northern bottlenose whales (*Hyperoodon ampullatus*) using the Gully, Nova Scotia. J Cetacean Res Manag 2:201–210

Gowans S, Whitehead HAL, Hooker SK (2001) Social organization in northern bottlenose whales, *Hyperoodon ampullatus*: Not driven by deep-water foraging? Anim Behav 62:369–377

Greene CH, Wiebe PH, Burczynski J, Youngbluth MJ (1988) Acoustical detection of high-density krill demersal layers in the submarine canyons off Georges Bank. Science 241:359–361

Guisan A, Zimmermann NE (2000) Predictive habitat distribution models in ecology. Ecol Modell 135:147–186

Hammond PS, Berggren P, Benke H, Borchers DL and others (2002) Abundance of harbour porpoise and other cetaceans in the North Sea and adjacent waters. J Appl Ecol 39:361–376

Hammond PS, Macleod K, Gillespie D, Swift R and others (2009) Cetacean offshore distribution and abundance in the European Atlantic (CODA): final report. University of St Andrews, St Andrews

Hammond PS, Macleod K, Berggren P, Borchers DL and others (2013) Cetacean abundance and distribution in European Atlantic shelf waters to inform conservation and management. Biol Conserv 164:107–122

Hastie T, Tibshirani R (1986) Generalized additive models. Stat Sci 1:297–318

Hátún H, Payne MR, Beaugrand G, Reid PC and others (2009) Large bio-geographical shifts in the north-eastern Atlantic Ocean: from the subpolar gyre, via plankton, to blue whiting and pilot whales. Prog Oceanogr 80:149–162

Hedley S, Buckland ST, Borchers D (1999) Spatial modeling from line transect data. J Cetacean Res Manag 1:255–264

Heide-Jørgensen MP, Blackwell SB, Tervo OM, Samson AL and others (2021) Behavioral response study on seismic airgun and vessel exposures in narwhals. Front Mar Sci 8:658173

Hooker SK (1999) Resource and habitat use of northern bottlenose whales in the Gully: ecology, diving and ranging behaviour. PhD dissertation, Dalhousie University, Halifax

Hooker SK, Baird RW (1999) Deep-diving behaviour of the northern bottlenose whale, *Hyperoodon ampullatus* (Cetacea: Ziphiidae). Proc R Soc B 266:671–676

Hooker SK, Whitehead H, Gowans S (1999) Marine protected area design and the spatial and temporal distribution of cetaceans in a submarine canyon. Conserv Biol 13:592–602

Hooker SK, Iverson SJ, Ostrom P, Smith SC (2001) Diet of northern bottlenose whales inferred from fatty-acid and stable-isotope analyses of biopsy samples. Can J Zool 79:1442–1454

Hooker SK, Whitehead H, Gowans S, Baird RW (2002) Fluctuations in distribution and patterns of individual range use of northern bottlenose whales. Mar Ecol Prog Ser 225:287–297

IHO–IOC (International Hydrographic Organization–Intergovernmental Oceanographic Commission) (2017) GEBCO Undersea Features Names Gazetteer. https://www.ngdc.noaa.gov/gazetteer/ (accessed 7 Aug 2017)

Isojunno S, Matthiopoulos J, Evans PGH (2012) Harbour porpoise habitat preferences: robust spatio-temporal inferences from opportunistic data. Mar Ecol Prog Ser 448:155–170

Kastelein RA, Gerrits NM (1991) Swimming, diving, and respiration patterns of a northern bottlenose whale (*Hyperoodon ampullatus*, Forster, 1770). Aquat Mamm 17:20–30

Kenny RD, Payne PM, Heinemann D, Winn HE (1996) Shifts in northeast shelf cetacean distributions relative to trends in Gulf of Maine/Georges Bank finfish abundance. In: Sherman K, Jaworski NA, Smayda T (eds) The northeast shelf ecosystem: assessment, sustainability, and management. Blackwell Science, Cambridge, p 169–196

Krausman PR (1999) Some basic principles of habitat use. In: Launchbaugh KL, Sanders KD, Mosley JL (eds) Grazing behaviour of livestock and wildlife. Idaho Forest, Wildlife and Range Experiment Station Bulletin No. 70, University of Idaho, Moscow, ID, p 85–90

Lick B, Piatkowski U (1998) Stomach contents of a northern bottlenose whale (*Hyperoodon ampullatus*) stranded at Hiddensee, Baltic Sea. J Mar Biol Assoc UK 78:643–650

Marques FFC, Buckland ST (2003) Incorporating covariates into standard line transect analyses. Biometrics 59:924–935

Marshall ML, David A, Miller L (2016) Package 'Distance'. https://cran.r-project.org/web/packages/Distance/Distance.pdf (accessed 27 Jan 2017)

Mellin C, Russell BD, Connell SD, Brook BW, Fordham DA (2012) Geographic range determinants of two commercially important marine molluscs. Divers Distrib 18:133–146

Michalsky J (1988) The Astronomical Almanac's algorithm for approximate solar position (1950–2050). Sol Energy 40:227–235

Miller PJO, Wensveen PJ, Isojunno S, Hansen R, Neves dos Reis M, Kleivane L (2014) Body condition project 2014 Jan Mayen Trial. Internal SMRU report. Sea Mammal Research Unit, St Andrews

Miller PJO, Kvadsheim PH, Lam FPA, Tyack PL and others (2015a) First indications that northern bottlenose whales are sensitive to behavioural disturbance from anthropogenic noise. R Soc Open Sci 2:140484

Miller PJO, Narazaki T, Isojunno S, Hansen R, Kershaw J, Neves dos Reis M, Kleivane L (2015b) Body condition and 3S15 projects: 2015 Jan Mayen trial. Internal SMRU report. Sea Mammal Research Unit, St Andrews

Miller PJO, Wensveen PJ, Isojunno S, Hansen R, Neves dos Reis M, Kleivane L (2016) $3S^3$ and body condition projects: 2016 Jan Mayen 2016 trial. Internal SMRU report. Sea Mammal Research Unit, St Andrews

NAMMCO (North Atlantic Marine Mammal Commission) (1995) NAMMCO Annual Report 1995. NAMMCO/5/6. North Atlantic Marine Mammal Commission, Tromsø. https://nammco.no/wp-content/uploads/2016/08/Annual-Report-1995.pdf

Øien N, Hartvedt S (2011) Northern bottlenose whales *Hyperoodon ampullatus* in Norwegian and adjacent waters. International Whaling Commission Scientific Committee document IWC/SC/63/SM1

Oschmann W (1991) Ecology and bathymetry of the late Quaternary shelly macribenthos from bathyal and abyssal areas of the Norwegian Sea. Senckenb Marit 21: 155–189

Piechura J, Walczowski W (1995) The Arctic Front: structure and dynamics. Oceanologia 37:47–73

Potts JM, Elith J (2006) Comparing species abundance models. Ecol Modell 199:153–163

R Core Team (2017) R: a language and environment for statistical computing. R Foundation for Statistical Computing, Vienna

Raj RP, Chatterjee S, Bertino L, Turiel A, Portabella M (2019) The Arctic Front and its variability in the Norwegian Sea. Ocean Sci 15:1729–1744

Ramírez-Martínez NC, Hammond PS (2019) Distribution and habitat use of deep-diving cetaceans in the central and north-eastern North Atlantic. NAMMCO Scientific Committee Abundance Estimation Working Group Document SC/26/AEWG/15

Redfern JV, Ferguson MC, Becker EA, Hyrenbach KD and others (2006) Techniques for cetacean–habitat modeling. Mar Ecol Prog Ser 310:271–295

Redfern JV, Barlow J, Bailance LT, Gerrodette T, Becker EA (2008) Absence of scale dependence in dolphin–habitat models for the eastern tropical Pacific Ocean. Mar Ecol Prog Ser 363:1–14

Reeves RR, Mitchell E, Whitehead H (1993) Status of the northern bottlenose whale, *Hyperoodon ampullatus.* Can Field Nat 107:490–508

Rogan E, Cañadas A, Macleod K, Santos B and others (2017) Distribution, abundance and habitat use of deep diving cetaceans in the North-East Atlantic. Deep Sea Res II 141:8–19

Santo E (2010) Community analysis of large epibenthos in the Nordic Seas. MSc dissertation, University of Iceland, Reykjavik

Shadish WR, Zuur AF, Sullivan KJ (2014) Using generalized additive (mixed) models to analyze single case designs. J Sch Psychol 52:149–178

Sivle LD, Kvadsheim PH, Curé C, Isojunno S and others (2015) Severity of expert-identified behavioural responses of humpback whale, mike whale, and northern bottlenose whale to naval sonar. Aquat Mamm 41:469–502

Skagseth Ø, Broms C, Gundersen K, Hátún H and others (2022) Arctic and Atlantic waters in the Norwegian Basin, between year variability and potential ecosystem implications. Front Mar Sci 9:831739

Smith RC, Dustan P, Au D, Baker KS, Dunlap EA (1986) Distribution of cetaceans and sea-surface chlorophyll concentrations in the California Current. Mar Biol 91: 385–402

Smith A, Hofner B, Lamb JS, Osenkowski J and others (2019) Modeling spatiotemporal abundance of mobile wildlife in highly variable environments using boosted GAMLSS hurdle models. Ecol Evol 9:2346–2364

Storrie L, Lydersen C, Andersen M, Wynn RB, Kovacs KM (2018) Determining the species assemblage and habitat use of cetaceans in the Svalbard Archipelago, based on observations from 2002 to 2014. Polar Res 37:1463065

Teloni V, Mark JP, Patrick MJO, Peter MT (2008) Shallow food for deep divers: dynamic foraging behavior of male sperm whales in a high latitude habitat. J Exp Mar Biol Ecol 354:119–131

Thomas R, Lello J, Medeiros R, Pollard A and others (2015) Data analysis with R statistical software: a guidebook for scientists. Eco-explore, Cardiff

Vetter EW, Dayton PK (1999) Organic enrichment by macrophyte detritus, and abundance patterns of megafaunal populations in submarine canyons. Mar Ecol Prog Ser 186:137–148

Vuong QH (1989) Likelihood ratio tests for model selection and non-nested hypotheses. Econometrica 57:307–333

Waring GT, Hamazaki T, Sheehan D, Wood G, Baker S (2001) Characterization of beaked whale (Ziphiidae) and sperm whale (*Physeter marocephalus*) summer habitat in shelf-edge and deeper waters off the Northwest US. Mar Mamm Sci 17:703–717

Wensveen PJ, Isojunno S, Hansen RR, Benda-Beckmann AMV and others (2019) Northern bottlenose whales in a pristine environment respond strongly to close and distant navy sonar signals. Proc R Soc B 286:20182592

Whitehead H, Hooker SK (2012) Uncertain status of the northern bottlenose whale *Hyperoodon ampullatus*: population fragmentation, legacy of whaling and current threats. Endang Species Res 19:47–61

Whitehead H, Reeves R, Feyrer L, Brownell JRL (2021) *Hyperoodon ampullatus*. The IUCN Red List of Threatened Species 2021:e.T10707A50357742. https://dx.doi.org/10.2305/IUCN.UK.2021-1.RLTS.T10707A50357742.en (accessed 25 Aug 2023)

Wiborg KF, Gjøsater J, Beck IM (1982) The squid *Gonatus fabricii* (Lichetenstein): investigations in the Norwegian Sea and western Barents Sea 1978–1981. ICES, Copenhagen

Wood SN (2006) Generalized additive models: an introduction with R. CRC Press, New York, NY

Wood S (2016) Package 'mgcv'. https://www.cran.r-project.org/web/packages/mgcv/mgcv.pdf (accessed 25 Jan 2017)

Zuur AF, Ieno EN, Walker NJ, Saveliev AA, Smith GM (2009) Zero-truncated and zero-inflated models for count data. In: Mixed effects models and extensions in ecology with R. Springer, New York, NY, p 261–293

Editorial responsibility: Lisa T. Ballance, Newport, Oregon, USA
Reviewed by: J. Stanistreet, S. Gowans

Submitted: December 18, 2022
Accepted: July 4, 2023
Proofs received from author(s): August 26, 2023